A Non-Hilbertian Inversion Technique for the Diagnosis of Faulty Elements in Antenna Arrays

Valentina Schenone[1], Alessandro Fedeli[1], Claudio Estatico[2], Matteo Pastorino[1], and Andrea Randazzo[1(✉)]

[1] Department of Electrical, Electronic, Telecommunications Engineering and Naval Architecture, University of Genoa, 16145 Genoa, Italy
valentina.schenone@edu.unige.it, {alessandro.fedeli, matteo.pastorino,andrea.randazzo}@unige.it
[2] Department of Mathematics, University of Genoa, 16146 Genoa, Italy
estatico@dima.unige.it

Abstract. Nowadays, antenna arrays are important tools adopted in a great number of applications including radar, mobile and satellite communication systems, and electromagnetic imaging. Moreover, in these applications, arrays with a high number of elements are ever more requested, which results in a growing possibility of damages in the array. The identification of defective components in array of antennas is really significant due to their applicative use: indeed, faulty detected elements can be fixed, thus avoiding to replace the whole antenna. In this work, a diagnostic technique for planar antenna arrays is presented. This approach enables recovering the eventually defective elements of the antenna under test using far-field data. To this end, an inversion approach established outside the standard context of Hilbertian spaces is used to address an inverse-source problem. A numerical validation concerning simple array antennas has been carried out to study the performances of the approach versus some antenna parameters, e.g., the size of the array.

Keywords: Diagnosis of antenna array · Inverse problems · Non-Hilbertian methods

1 Introduction

Arrays of antennas have a wide variety of applications, including telecommunications and microwave imaging [1–5]. Indeed, their main benefit is the capability to fit their radiation properties to the framework in which they operate.

In this scenario, antenna diagnosis is fundamental to identify defects that might result in changes of the radiated fields required by the specific application. Furthermore, current applications often require arrays composed by a high number of antennas. This increases the probability of faulty elements occurrences and makes their identification and replacement a very important task.

M. Valle et al. (Eds.): SYSINT 2022, LNNS 546, pp. 173–181, 2023.
https://doi.org/10.1007/978-3-031-16281-7_17

The antenna array diagnosis may be considered an inverse problem: measured far-field data are used to reconstruct the distribution of currents (or the corresponding feed coefficients) on the inspected antenna [6]. However, this problem requires to face ill-posed equations. Many solutions have been offered by the current scientific research to cope with such an inverse problem. For instance, methods relying upon the so-called equivalent source reconstruction method to reconstruct an equivalent currents distribution through Huygens' principle have been proposed [7–9]. Compressive sensing (CS)-based approaches were also presented [10–14], assuming that failures belong to a sparse distribution.

A new diagnostic approach is devised in this paper to extract the excitations of damaged antennas. This procedure relies on an non-Hilbertian spaces-based technique to perform inversion in a regularized way [15–17]. This family of methods has been able to produce promising reconstruction outcomes with an appropriate tweaking of the exponent function, which allows enforcing sparsity without that sparseness conditions are severely fulfilled [18, 19]. This technique brings some advantages over existing methods. Indeed, as regards procedures based on compressive sensing, they allow obtaining good reconstructions but mainly in the case of sparse solutions. Furthermore, in order to apply these techniques, some specific conditions need to be met, the so-called RIP conditions [10, 18, 19]. On the contrary, inversion in non-Hilbertian spaces frees users from the need to check the RIP conditions. It is also worth mentioning the approaches formulated in the classic Hilbert spaces. The use of these techniques often leads to solutions characterized by significant smoothing effects, which therefore are not suitable for the reconstruction of sparse defects. In this sense, the non-Hilbertian strategy makes it possible to restore different types of solutions, through an appropriate adaptation of the exponent function. The approach is validated through numerical simulations concerning antenna arrays under test of different sizes. More in details, a study has been conducted with two percentage of faulty elements for each size of antenna array.

This contribution is structured as follows. Section 2 presents the involved inverse-source problem and discusses the solving strategy. In Sect. 3, the devised solving methodology is assessed in a numerically simulated framework. At the end, conclusions are given in Sect. 4.

2 Mathematical Formulation

In Fig. 1 the analyzed antenna diagnostic configuration is sketched, where $S = S_x \times S_y$ antennas are centered at points (x_s, y_s). The spacings between antenna elements are δ_x (on the x axis) and δ_y (on the y axis). A working angular frequency ω_0 is considered.

The developed procedure detects eventually present faulty elements from measurements of the radiated electric far-field. In particular, a reference planar array is considered with $\boldsymbol{a}$ being the vector of element feed excitations. As concerns the antenna under test (AUT), it is supposed to have $S_h = hS$ faulty elements in the array (h the percentage of failure) and $\hat{\boldsymbol{a}}$ is the vector of the AUT excitations. Two vectors $\boldsymbol{F}$ and $\widehat{\boldsymbol{F}}$ are obtained for reference array and AUT by measuring the components of the radiated field in D points (θ_d, φ_d), in the far field region. These measurements are collected with an angular interval between measurement points of $\Delta\theta = \Delta\varphi$ and $0 \leq \theta \leq \frac{\pi}{2}$, $0 \leq \varphi < 2\pi$.

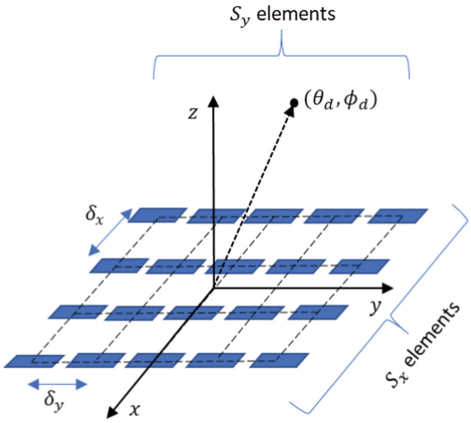

Fig. 1. Sketch of the considered array of antennas.

The radiated far field pattern at the measurement points (θ_d, φ_d), for $d = 1, \ldots, D$, can be written as [20]

$$F^{\boldsymbol{c}}(\theta_d, \varphi_d) = \sum_{s=1}^{S} a_s E^c_{sd}(\theta_d, \varphi_d) e^{j\frac{2\pi}{\lambda}(x_s sin\theta_d cos\varphi_d + y_s sin\theta_d sin\varphi_d)} \tag{1}$$

where $c = \{\theta/\varphi\}$ represents the θ/φ-pattern component and E^c_{sd} represents the embedded pattern for the antenna s in (θ_d, φ_d) [13, 21], which is the array's far-field pattern when the antenna s is stimulated with unitary excitation while other antennas are matched. By combining all the available D observation directions with reference and faulty array measurements, a linear system, which joins the vector $\boldsymbol{H} = \boldsymbol{F} - \widehat{\boldsymbol{F}}$ with the unknown vector of faulty feed coefficients $\boldsymbol{b} = \boldsymbol{a} - \widehat{\boldsymbol{a}}$, is obtained, i.e.,

$$\boldsymbol{H} = [M]\boldsymbol{b} \tag{2}$$

where $[M]$ is an $D \times S$ matrix with elements given by $[M]_{sd} \triangleq E^c_{sd}(\theta_d, \varphi_d) e^{j2\pi(x_s sin\theta_d cos\varphi_d + y_s sin\theta_d sin\varphi_d)/\lambda}$. Therefore, each coefficient of the matrix can be obtained knowing a-priori the array geometry and the embedded pattern measurement for each antenna in the array. It is worth noting that $\boldsymbol{b}$ has zero-value in correspondence of non-faulty elements, whereas non-zero coefficients reveal a damaged antenna and their value provide information about fault entity. Thus, the diagnosis is performed by inverting this equation and recovering $\boldsymbol{b}$.

To this end, a regularization strategy in L^p spaces based on the truncated Landweber algorithm is proposed to solve the inverse problem [22–24]. Specifically, this is an iterative method where, after defining an initial value $\boldsymbol{b}_0$ (e.g., $\boldsymbol{b}_0 = 0$ if no a-priori information is available), at each iteration the solution is updated as follows:

$$\boldsymbol{b}_{k+1} = \mathrm{J}_q\{\mathrm{J}_p(\boldsymbol{b}_k) - \alpha[M]^* \mathrm{J}_p([M]\boldsymbol{b}_k - \boldsymbol{H})\} \tag{3}$$

where $\alpha > 0$ defines the length of each step and is equal to $\alpha = 1/4\left\{1/\|[M]\|_1^2 + (p-1)\left(1/\|[M]\|_2^2 - 1/\|[M]\|_1^2\right)\right\}$, $[M]^*$ is the adjoint of $[M]$, that

is under the examined situations, the Hermitian transposition, and $q = p(p-1)^{-1}$ is the Hölder conjugate of p. The key elements in the truncated Landweber-like method formulated in non-Hilbertian L^p spaces are the so-called duality maps of the L^p space, J_p, used to associate a vector $\boldsymbol{x}$ to its corresponding vector in the dual space, whose l-component is given by $\left\{\mathrm{J}_p(\boldsymbol{x})\right\}_l = |x_l|^{p-1}\mathrm{sign}(x_l)\|\boldsymbol{x}\|_{L^p}^{2-p}$ [22]. In this way, the approach minimizes the residual $R(\boldsymbol{b}_k) = 0.5\|[M]\boldsymbol{b}_k - \boldsymbol{H}\|_p^2$ by moving along non-standard gradient directions in the dual space. The step reported in Eq. (3) is repeated for $k = 0, 1, \ldots, K$ and until a predefined halting criterion is met.

3 Results of Numerical Simulations

A numerical framework has been adopted to validate the devised diagnostic approach. A planar antenna array with one-parameter Taylor excitations is simulated with a sidelobe level equal to $R = 25$ dB [25]. Besides, ideal isotropic antennas are considered, with $\delta_x = \delta_y = \lambda/2$ ($\lambda = 0.15\,m$). $D = 325$ far-field points are considered, with $\Delta\theta = \Delta\varphi = \pi/18$. A zero mean value Gaussian noise with $SNR = 25$ dB is used to corrupt the synthetic data. Moreover, as regards the antenna under test, total failures randomly distributed in the array are considered (i.e., $a_s = 0$ if element s is faulty).

The relative recovery error on the reconstructed vector of faulty feed coefficients, defined as:

$$e_{rec} = \frac{\|\tilde{\boldsymbol{b}} - \boldsymbol{b}^*\|_1}{\|\boldsymbol{b}^*\|_1} \tag{4}$$

where $\tilde{\boldsymbol{b}}$ and $\boldsymbol{b}^*$ stand for the vectors of the recovered and actual faulty feed coefficients, respectively, has been used to assess the correctness of the diagnosis.

Arrays with equal number of elements along the x-axis and y-axis, i.e., $S_x = S_y = N$, are considered, and the behavior of the method versus the parameter p is studied for $1.1 \leq p \leq 2.0$ with numbers of array elements in the range $N \in [15, 20]$. Such a range for the norm parameter has been selected starting from values of p close to 1, which have been demonstrated in imaging application to be useful for sparse solution [15, 16] and choosing as upper bound $p = 2$, which represents the classical method in Hilbert spaces. This study has been accomplished for percentage of failure $h = 0.1$ and $h = 0.3$. As concerns method parameters, the method is stopped when reaches the minimum normalized root mean square error, and $K = 10000$ has been fixed as the upper bound for iteration number.

The values of e_{rec} versus the exponent parameters p achieved by the developed method with $h = 0.1$ are shown in Fig. 2. In this case, the error is minimum for $p = 1.1$ and then increases for higher values of p. Regarding the variation on array dimensions, as can be noticed, by considering the best recovery error, good reconstructions are achieved for all the arrays. In Fig. 3, two cases of the recovered magnitude of the failure vectors of the examined antenna, obtained with the best value of the exponent parameter ($p = 1.1$), are shown. Such figures confirm that the developed inversion strategy enables a good identification of faulty elements. Moreover, the values of the amplitude of the vector of faulty feed coefficients are very close to the actual ones.

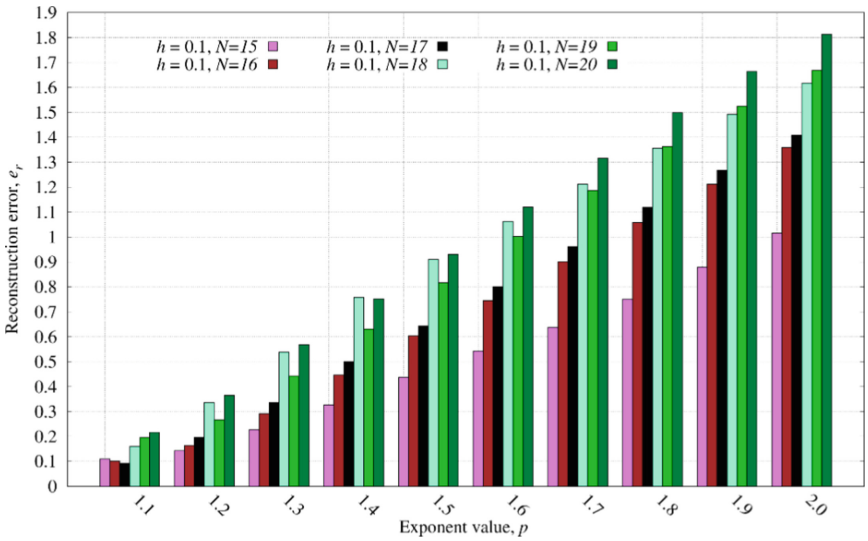

Fig. 2. Relative recovery error for a percentage of failure $h = 0.1$, with array dimension parameter $N \in [15, 20]$ and norm parameter $p \in [1.1, 2]$.

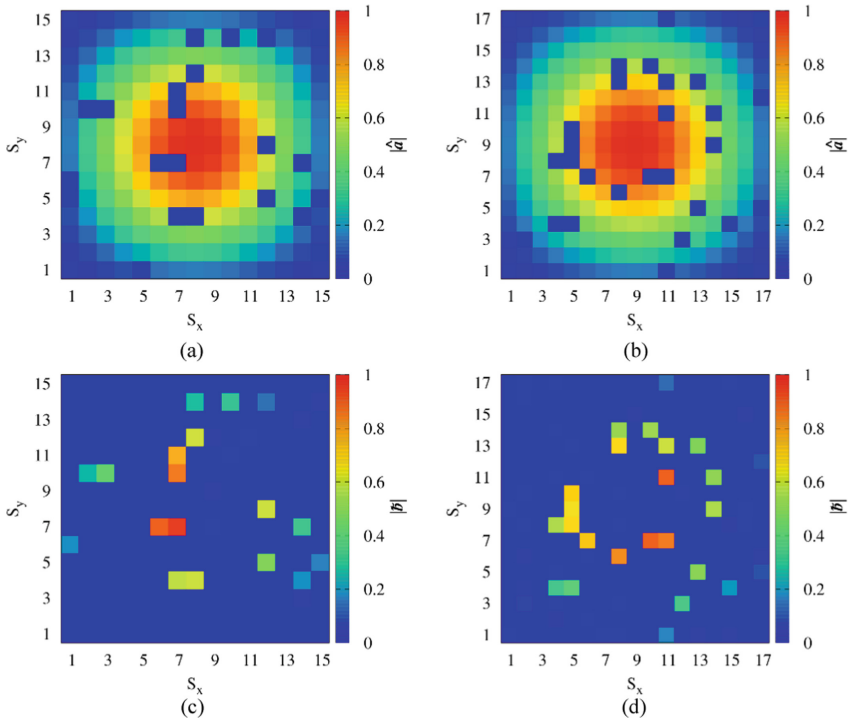

Fig. 3. Feed coefficients magnitude of the damaged antenna for $h = 0.1$ and (a) $N = 15$ and (b) $N = 17$ elements. Best recovered vector of faulty feed coefficients magnitude for (c) $N = 15$ and (d) $N = 17$.

Figure 4 displays the values of e_{rec} against p and the number of array elements with $h = 0.3$. As can be seen, the error has a minimum for a value of $p \in [1.2, 1.3]$ and then it rises again with greater values of p. In this case, by increasing the array dimension, the optimum value of p slightly increases (for $N = 20$, $p = 1.3$). Moreover, a worsening in the reconstruction can be observed as the array dimension increases, since a higher and higher number of non-zero elements has to be reconstructed. Figure 5 shows the magnitude of the actual feed coefficients of the inspected antenna and the best recovered vector of faulty feed coefficients (obtained by setting $p = 1.2$) for $N = 15$ and $N = 17$.

By this analysis, it can be concluded that lower p values enable a good reconstruction when few faulty elements are present (as it happens when $h = 0.1$ and large array are considered), whereas higher values of $p \in [1.2, 1.3]$ perform better for the recovery of unknowns with higher numbers of non-zero elements ($h = 0.3$ and quite large array). This result is consistent with the intrinsic sparsity enhancement of all the methods which minimize the L1 norm of the solution. In our proposal, $p > 1$ exponents close to 1 allow obtaining sparse solutions, while larger values of p are more suited for non-sparse restorations. Therefore, by this study it is evident how this approach allows reconstructing both sparse and non-sparse solutions through an adequate selection of the exponent parameter (differently from the methods relying upon compressive sensing) and without the need of fulfilling the RIP condition. Besides, by comparing the best solution with those achieved with $p = 2.0$, which coincides with the regularization in the classic Hilbert spaces, it can be observed that this technique enables to get better results for all the analyzed cases.

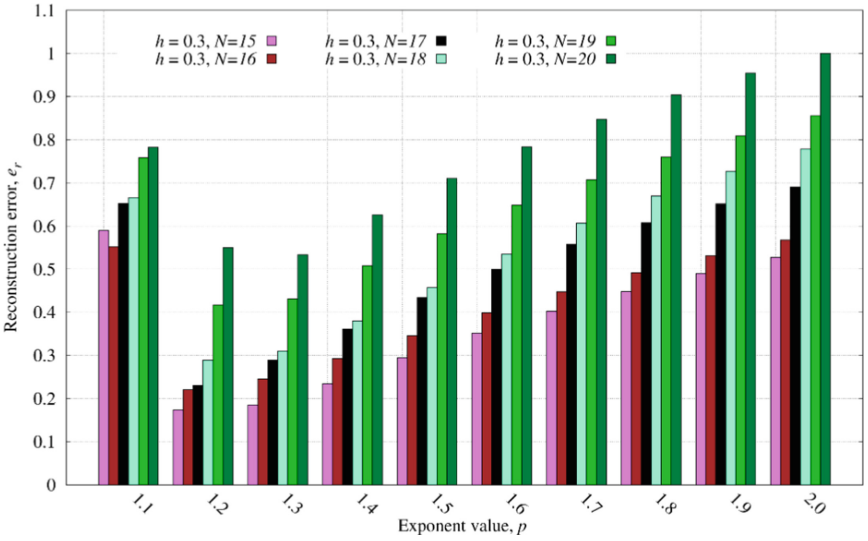

Fig. 4. Relative recovery error for a percentage of failure $h = 0.3$, array dimension parameter $N \in [15, 20]$ and norm parameter $p \in [1.1, 2]$.

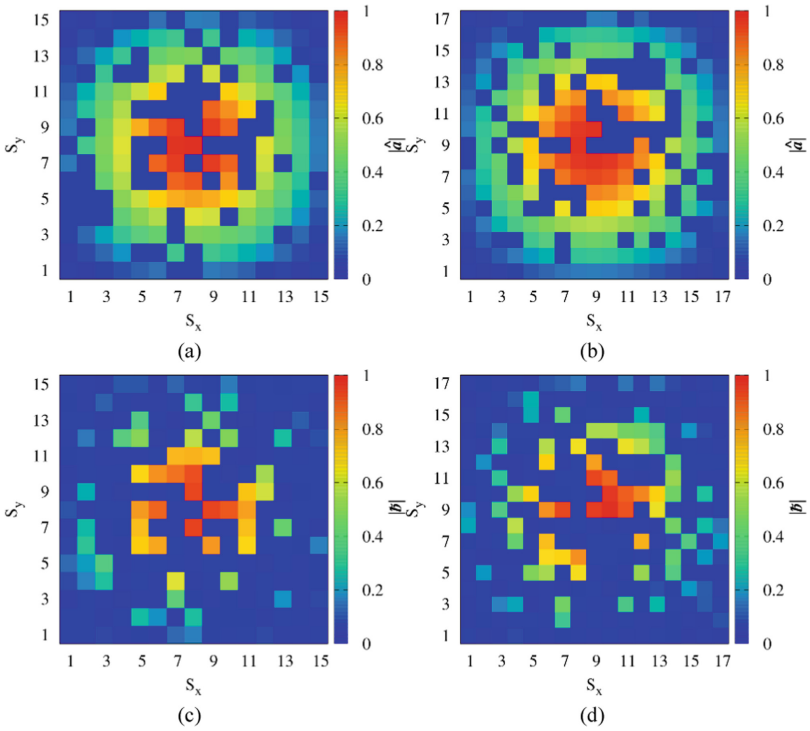

Fig. 5. Feed coefficients magnitude of the damaged antenna for $h = 0.3$ and for (a) $N = 15$ and (b) $N = 17$. Best recovered vector of faulty feed coefficients magnitude (c) $N = 15$, (d) $N = 17$.

4 Conclusion

An antenna array diagnosis method, which aims at solving an inverse-source problem to reconstruct the presence of defective antenna elements in arrays, has been proposed in the present work. In details, a procedure based on the Landweber method in non-Hilbertian L^p spaces was developed to solve the problem at hand in a regularized fashion. Numerical experiments were performed to test the proposed methodology, including a variation of the array size and of the exponent parameter p, considering the test case of a planar antenna array. By fine-tuning the p parameter, accurate diagnostic results can be produced. A comprehensive numerical evaluation of the method and the validation in more realistic settings will be part of future advancements.

Acknowledgements. This work was partially supported by the Italian Ministry for Education, University, and Research under the project PRIN2017 DI-CA, grant number 20177C3WRM.

References

1. Chen, Y., Zhou, W., Yang, S.: Design of a low-profile and low scattering wideband planar phased antenna array. IEEE Trans. Antennas Propag. 69, 8973–8978 (2021)

2. Ahmed, A., Zhang, Y., Burns, D., Huston, D., Xia, T.: Design of UWB antenna for air-coupled impulse ground-penetrating radar. IEEE Geosci. Remote Sens. Lett. **13**, 92–96 (2016)
3. Leone, G., Munno, F., Pierri, R.: Radiation of a circular arc source in a limited angle for nonuniform conformal arrays. IEEE Trans. Antennas Propag. **69**, 4955–4966 (2021)
4. Abbak, M., Nuri Akıncı, M., Ertay, A.O., Özgür, S., Işık, C., Akduman, İ: Wideband compact dipole antenna for microwave imaging applications. IET Microwaves Antennas Propag. **11**, 265–270 (2017)
5. Zeitler, A., Lanteri, J., Pichot, C., Migliaccio, C., Feil, P., Menzel, W.: Folded reflectarrays with shaped beam pattern for foreign object debris detection on runways. IEEE Trans. Antennas Propag. **58**, 3065–3068 (2010)
6. Leone, G., Maisto, M.A., Pierri, R.: Application of inverse source reconstruction to conformal antennas synthesis. IEEE Trans. Antennas Propag. **66**, 1436–1445 (2018)
7. Alvarez, Y., Las-Heras, F., Pino, M.R.: The sources reconstruction method for amplitude-only field measurements. IEEE Trans. Antennas Propag. **58**, 2776–2781 (2010)
8. Konno, K., Asano, S., Umenai, T., Chen, Q.: Diagnosis of array antennas using eigenmode currents and near-field data. IEEE Trans. Antennas Propag. **66**, 5982–5989 (2018)
9. Tzoulis, A., Eibert, T.F.: A hybrid FEBI-MLFMM-UTD method for numerical solutions of electromagnetic problems including arbitrarily shaped and electrically large objects. IEEE Trans. Antennas Propag. **53**, 3358–3366 (2005)
10. Fuchs, B., Coq, L.L., Migliore, M.D.: Fast antenna array diagnosis from a small number of far-field measurements. IEEE Trans. Antennas Propag. **64**, 2227–2235 (2016)
11. Xiong, C., Xiao, G., Hou, Y., Hameed, M.: A compressed sensing-based element failure diagnosis method for phased array antenna during beam steering. IEEE Antennas Wirel. Propag. Lett. **18**, 1756–1760 (2019)
12. Ince, T., Ögücü, G.: Array failure diagnosis using nonconvex compressed sensing. IEEE Antennas Wirel. Propag. Lett. **15**, 992–995 (2016)
13. Salucci, M., Gelmini, A., Oliveri, G., Massa, A.: Planar array diagnosis by means of an advanced Bayesian compressive processing. IEEE Trans. Antennas Propag. **66**, 5892–5906 (2018)
14. Palmeri, R., Isernia, T., Morabito, A.F.: Diagnosis of planar arrays through phaseless measurements and sparsity promotion. IEEE Antennas Wirel. Propag. Lett. **18**, 1273–1277 (2019)
15. Estatico, C., Fedeli, A., Pastorino, M., Randazzo, A.: Microwave imaging of elliptically shaped dielectric cylinders by means of an Lp Banach-space inversion algorithm. Meas. Sci. Technol. **24**, 074017 (2013)
16. Estatico, C., Fedeli, A., Pastorino, M., Randazzo, A., Tavanti, E.: A phaseless microwave imaging approach based on a Lebesgue-space inversion algorithm. IEEE Trans. Antennas Propag. **68**, 8091–8103 (2020)
17. Fedeli, A., Schenone, V., Randazzo, A., Pastorino, M., Henriksson, T., Semenov, S.: Nonlinear S-parameters inversion for stroke imaging. IEEE Trans. Microw. Theory Tech. **69**, 1760–1771 (2021)
18. Massa, A., Rocca, P., Oliveri, G.: Compressive Sensing in Electromagnetics - A Review. IEEE Antennas Propag. Mag. **57**, 224–238 (2015)
19. Tipping, M.E.: Sparse bayesian learning and the relevance vector machine. J. Mach. Learn. Res. **1**, 211–244 (2001)
20. Balanis, C.A.: Antenna theory: Analysis and design. John Wiley & Sons, Hoboken, NJ (2016)
21. Kelley, D.F., Stutzman, W.L.: Array antenna pattern modeling methods that include mutual coupling effects. IEEE Trans. Antennas Propag. **41**, 1625–1632 (1993)
22. Estatico, C., Pastorino, M., Randazzo, A.: A novel microwave imaging approach based on regularization in Lp Banach spaces. IEEE Trans. Antennas Propag. **60**, 3373–3381 (2012)

23. Brianzi, P., Di Benedetto, F., Estatico, C.: Improvement of space-invariant image deblurring by preconditioned Landweber iterations. SIAM J. Sci. Comput. **30**, 1430–1458 (2008)
24. Fedeli, A., Pastorino, M., Ponti, C., Randazzo, A., Schettini, G.: Through-the-Wall Microwave Imaging: Forward and Inverse Scattering Modeling. Sensors. **20**, 2865 (2020)
25. Orfanidis, S.J.: Electromagnetic Waves and Antennas (2016). http://www.ece.rutgers.edu/~orfanidi/ewa/